

## A-type potassium channels expressed from Shaker locus cDNA

L. E. IVERSON\*, M. A. TANOUYE\*, H. A. LESTER\*, N. DAVIDSON†, AND B. RUDY‡§

Divisions of \*Biology and †Chemistry, California Institute of Technology, Pasadena, CA 91125; and ‡Department of Physiology and Biophysics, New York University Medical Center, 550 First Avenue, New York, NY 10016

Contributed by N. Davidson, April 1, 1988

**ABSTRACT** A-type  $K^+$  currents are expressed in *Xenopus* oocytes injected with *in vitro*-synthesized transcripts from cDNAs for the *Drosophila* Shaker (*Sh*) locus. A single *Sh* gene product, possibly as a multimer, is sufficient for formation of functional A channels. Various *Sh* RNAs express A currents with distinct kinetic properties. An analysis of structure–function relationships shows that the conserved central region of *Sh* polypeptides determines ionic selectivity and overall channel behavior, whereas the divergent amino and carboxyl termini can modify channel kinetics. Alternative splicing of *Sh* gene transcripts may provide one mechanism for the generation of  $K^+$  channel diversity.

$K^+$  channels are a ubiquitous and extraordinarily diverse group of ion channels that play a major role in controlling excitability properties of nerve and muscle (1, 2); they are also important to non-neuronal cell physiology (2). In the nervous system,  $K^+$  channels contribute to the determination of resting potentials, to the duration of action potentials, to the generation of diverse firing patterns, and to some forms of learning (2–5). Despite their importance in nervous system function, virtually nothing was known about the structure of  $K^+$  channel proteins or the molecular basis for  $K^+$  channel diversity.

Several lines of evidence suggest that the *Drosophila* Shaker (*Sh*) locus is the structural gene for a  $K^+$  channel. *Sh* mutations specifically alter a fast, transient, voltage-sensitive, A-type (A1)  $K^+$  current in muscle (6–9). Structural features of predicted *Sh* gene products provide additional evidence that *Sh* encodes a  $K^+$  channel; the deduced amino acid sequence of *Sh* cDNAs reveals a number of hydrophobic domains indicative of a membrane-spanning protein (10–14), and several *Sh* gene products contain a sequence similar to a putative amphipathic helix (S4 region) believed to be involved in gating of the voltage-dependent  $Na^+$  channel (15–17). In addition, sequence analysis of *Sh* cDNAs indicates that *Sh* encodes a number of distinct transcripts that arise by an alternative splicing mechanism (13, 14) that may account for the diversity among some  $K^+$  channels.

In this study we provide direct evidence that *Sh* is the structural gene for a  $K^+$  channel by showing that transcripts synthesized *in vitro* from *Sh* cDNAs express A-type  $K^+$  currents when injected into *Xenopus* oocytes. Our results, and the results reported by Timpe *et al.* (18), indicate that at least three functionally distinct  $K^+$  currents are expressed from different *Sh* transcripts. These studies provide insight into the molecular basis of  $K^+$  channel diversity and a preliminary description of the structural elements that control functional properties of  $K^+$  channels.

### MATERIALS AND METHODS

***In Vitro* Synthesis of RNA.** Recombinant Bluescript (Stratagene, San Diego, CA) plasmids containing *Sh* cDNA inserts

were linearized by digestion with the appropriate restriction enzymes. Template DNA was incubated with the appropriate RNA polymerase (T7 or T3) to synthesize full-length capped transcripts (19).

**RNA Injections and Electrophysiological Techniques.** *Xenopus laevis* oocytes were injected with RNA and incubated for 2–3 days at 22°C in ND96 (96 mM NaCl/2 mM KCl/1.8 mM  $CaCl_2$ /1 mM  $MgCl_2$ /5 mM Hepes, pH 7.5) supplemented with penicillin (100 units/ml), streptomycin (100  $\mu$ g/ml), and 2.5 mM sodium pyruvate. Macroscopic currents were recorded in ND96 with a standard two-microelectrode voltage clamp (20). Single-channel records were obtained with the outside-out configuration of the patch clamp technique (20). Bath solution was ND96; and pipettes were filled with 90 mM KCl/10 mM NaCl/10 mM EGTA/10 mM Hepes, pH 7.4. All experiments, except where otherwise indicated, were carried out at room temperature (19–22°C).

### RESULTS

**Injection of *Sh* RNA Induces Transient, Outward Currents in *Xenopus* Oocytes.** The general structure of the *Sh* cDNAs consists of a conserved central region flanked by variable 5' and 3' ends (11, 13, 14). At least three distinct 5' ends (I–III) and four 3' ends (i–iv) have been described (13). The 5' and 3' ends appear to assort independently yielding at least 12 possible combinations. Protein coding regions initiate in the variable 5' domains, extend through the constant region, and terminate in the variable 3' domains, yielding a group of similar proteins with distinct amino and carboxyl termini. *Sh* cDNAs with class i, ii, or iv 3' ends predict proteins with six hydrophobic domains and one S4-like sequence. The sequence identity of these cDNAs extends beyond the constant region up to the middle of the fifth hydrophobic domain. In contrast, the coding region of *Sh* cDNAs with class iii 3' ends terminates immediately after the constant region yielding proteins with three hydrophobic domains and no S4-like sequence. Fig. 1A depicts structural features of the four *Sh* cDNAs used in this report.

Transient outward currents resembling A currents (Fig. 1C–F) were observed in oocytes injected with H4 and H37 transcripts synthesized *in vitro* (Fig. 1B); injection of E1 and H2 transcripts failed to produce any response (data not shown). Current–voltage plots (Fig. 1G) show that currents in cells injected with H4 and H37 RNAs start to activate at membrane potentials between –40 and –30 mV, similar to values reported for A channels in *Drosophila* muscle (6–9).

**Currents Are Carried by  $K^+$ .** The reversal potential of the currents expressed in oocytes injected with *Sh* RNAs depends on the external  $K^+$  concentration as expected for a  $K^+$ -selective channel (Fig. 2). Fig. 2A shows tail currents recorded from an oocyte expressing H4 RNA bathed in 10 mM KCl. The current–voltage relationship (Fig. 2B) shows that the current reverses at about –50 mV, similar to the

The publication costs of this article were defrayed in part by page charge payment. This article must therefore be hereby marked "advertisement" in accordance with 18 U.S.C. §1734 solely to indicate this fact.

§To whom reprint requests should be addressed.

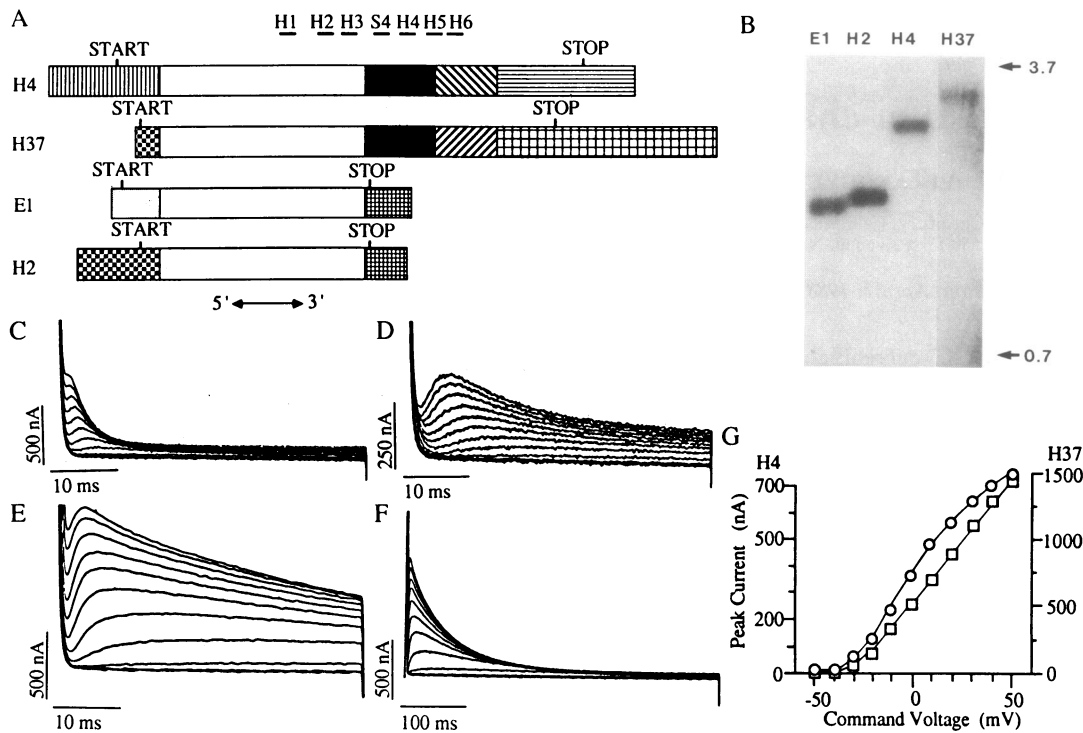


FIG. 1. Expression of transient outward currents in *Xenopus* oocytes injected with transcripts of Sh cDNAs synthesized *in vitro*. (A) Sh cDNAs used in transcription reactions. Similar shadings reflect identical DNA sequences of 5' and 3' variable and conserved central domains. Positions of the translational start and stop codons, the six hydrophobic domains (H1–H6), and the amphipathic S4 region are indicated. For additional details see Kamb *et al.* (13). (B)  $^{32}\text{P}$ -labeled RNA samples (2000 cpm), transcribed *in vitro*, were denatured by heating for 15 min at 55°C in 50% (vol/vol) formamide and then electrophoresed on a 1% agarose/6.6% formaldehyde gel alongside  $^{32}\text{P}$ -labeled  $\lambda$  *Bst* EII DNA fragments. An autoradiogram of the gel is shown. Position of the DNA size standards (in kilobases) are indicated by the arrows. Single RNA bands of the expected size for full-length transcripts are observed. (C–F) Ion currents recorded in oocytes injected with H4 (C and D) or H37 (E and F) RNA with a two-microelectrode voltage clamp. The membrane potential was held at  $-90$  mV followed by a 1-s hyperpolarizing prepulse to  $-120$  mV, then stepped to test potentials ranging from  $-50$  to  $+50$  mV in 10 mV increments. Test pulses were applied at a frequency of one every 5 s for H4- and one every 30 s for H37-injected oocytes. Only the currents during the test depolarizations are shown here. Currents in C, E, and F were recorded at 20°C or in D at 10°C. From this experiment we calculate a  $Q_{10}$  for both activation and inactivation of 3.2. Note that there is also a significant effect of temperature on current magnitude;  $Q_{10}$  is 2. (G) Peak currents from the experiments in C (H4,  $\square$ ) and E (H37,  $\circ$ ) are plotted as a function of membrane potential after leak subtraction. Note the different scales.

expected reversal potential of  $-53$  mV in the experimental ionic conditions. Reversal potentials plotted as a function of external  $\text{K}^+$  concentration show a slope of 48 mV change in reversal potential for a 10-fold change in external  $\text{K}^+$  concentration (Fig. 2C). This is close to the 56 mV change predicted by the Nernst equation for a  $\text{K}^+$ -selective channel.

Tail current studies from cells expressing H37 RNA yielded similar results (data not shown).

The pharmacology of the channels expressed in oocytes also suggests that Sh cDNAs encode  $\text{K}^+$  channels. Greater than 50% reduction in current amplitude was observed in Sh RNA injected oocytes bathed in 2 mM 4-aminopyridine; the

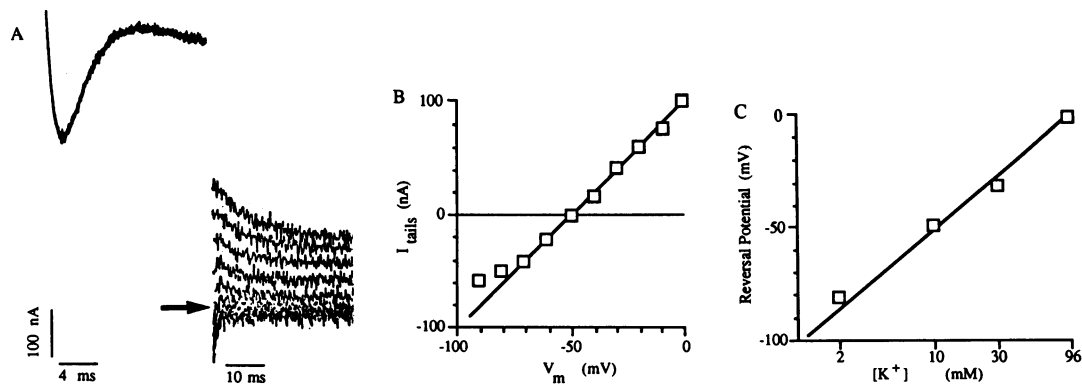


FIG. 2. Transient, outward currents are carried by  $\text{K}^+$ . (A) Tail currents recorded in 10 mM KCl at 12°C in an oocyte injected with H4 RNA. The membrane potential was held at  $-90$  mV then stepped to  $+40$  mV for 15 ms (upper traces). Before the current inactivated, the membrane potential was stepped down to levels from  $-90$  to 0 mV in 10-mV increments, and tail currents were recorded at these potentials (lower traces). The tail currents are inward at negative potentials and outward at positive potentials. The arrow indicates the point at which the current reversed direction (the reversal potential). (B) The initial amplitude of the tail currents in A was determined by extrapolating the currents to the beginning of the pulse. The difference between this value and the steady-state value is plotted as a function of the test potential. The current is 0 at  $-50$  mV (the reversal potential). (C) Reversal potentials, obtained from several different determinations as described above, are plotted as a function of the external  $[\text{K}^+]$ . In all cases the KCl concentration was increased at the expense of NaCl.

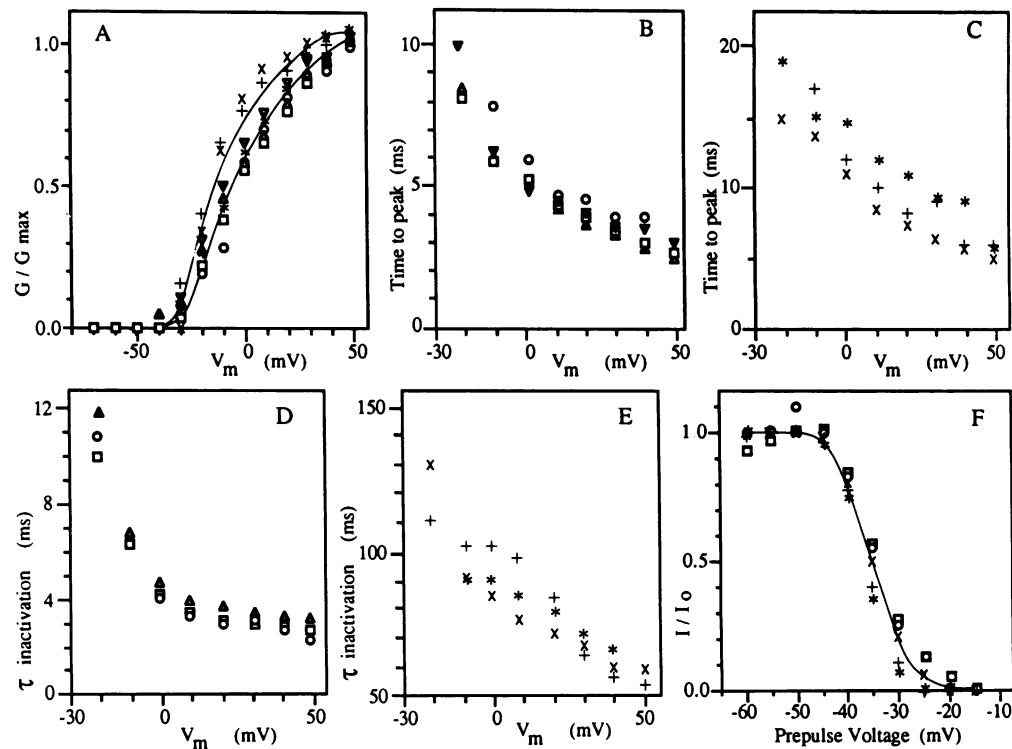


FIG. 3. Comparison of the current properties at room temperature from several oocytes injected with either H4 ( $\circ$ ,  $\square$ ,  $\Delta$ , or  $\nabla$ ) or H37 ( $+$ ,  $\times$ , or  $*$ ) RNA. (A) The relative peak conductance was determined by dividing the conductance at the indicated potentials by the conductance at +50 mV. The conductance was determined from the equation  $G = I/V_m - V_K$ , assuming a  $V_K = -80$  mV. (B and C) Time required for the currents from cells expressing H4 (B) and H37 (C) RNAs to reach maximum levels (time to peak) plotted as a function of test potential. (D and E) Time constants of inactivation of the currents from cells expressing H4 (D) and H37 (E) RNAs plotted as a function of the indicated membrane potentials. The time constants were obtained by fitting the decay of the current during a test pulse to a single exponential and a steady state. (F) Steady-state inactivation of currents induced in cells expressing H4 ( $\circ$ ,  $\square$ ) and H37 ( $+$ ,  $\times$ , or  $*$ ) RNA. The membrane potential was held at  $-90$  mV followed by 1-s prepulses to the indicated voltages then stepped to a test pulse of +30 mV, and the peak current was measured. The ratio ( $I/I_0$ ) of the peak current obtained during this test pulse ( $I$ ) to the peak current obtained during a test pulse to +30 mV after a prepulse to  $-120$  mV ( $I_0$ ) is plotted as a function of the prepulse potential. The curve, the best fit of the experimental data to a Boltzman distribution, has a slope of 4.5 mV change for every  $e$ -fold change in steady-state inactivation and a midpoint of  $-35$  mV.

currents were completely blocked in 5 mM 4-aminopyridine (data not shown). Externally applied 4-aminopyridine blocks several types of  $K^+$  channels (1), including A channels in *Drosophila* muscle (7, 9).

Thus, the transient character, voltage-dependent activation,  $K^+$  selectivity, and pharmacology indicate that the currents expressed in oocytes injected with Sh RNA are similar to *Drosophila* muscle A currents. These results demonstrate that a single Sh gene product is sufficient to produce functional A channels in the oocyte membrane.

**Various Sh RNAs Expressed  $K^+$  Currents with Similar Voltage Dependence but with Distinct Kinetics.** We have shown above that currents from cells expressing H4 and H37 RNAs are similar in their voltage dependence of activation,  $K^+$  selectivity, and sensitivity to 4-aminopyridine. Conductance-voltage curves for currents from cells expressing H4 and H37 RNAs from several experiments (Fig. 3A) confirm that the voltage dependence of channel opening is similar. Steady-state inactivation curves of the two currents are also similar both in their steepness and position on the voltage scale indicating a similar voltage dependence of macroscopic inactivation (Fig. 3F).

However, the currents have different kinetic properties. This is particularly evident for the rate of current decay during constant depolarization (Fig. 1C and E). A comparison of the times to peak and the inactivation rates (Fig. 3B-E) indicates that H37 channels both activate and inactivate significantly slower than H4 channels at all voltages. In addition, the currents from cells expressing H4 and H37 RNAs also differ markedly in the time required to recover from inactivation. The current from cells expressing H4 RNA

recovers relatively quickly from inactivation at a membrane potential of  $-100$  mV (Fig. 4A). Recovery does not proceed with a single exponential time course; 50% of the current is recovered in 25 ms at  $19-21^\circ\text{C}$  and 95% in 165 ms. In contrast, only 70% of the current from cells expressing H37 RNA recovers in 1.5 s at  $-100$  mV, the remaining current recovers very slowly at this potential (Fig. 4B). Recovery is significantly slower at membrane potentials more positive than  $-100$  mV. For example, at potentials closer to a typical neuronal resting potential of  $-70$  to  $-60$  mV, complete recovery of the current from cells expressing H37 RNA requires  $>1$  min (data not shown).

**Single-Channel Analysis of Sh  $K^+$  Channels.** Fig. 5A illustrates single channel currents recorded in outside-out patches from oocytes injected with H4 RNA. Some sweeps show one channel opening followed by channel closure for the duration of the test pulse. Although most channels open early, the delay to first opening (first latency) varies widely. Occasionally a second opening is observed during a single test pulse. Less frequently we observe channels that remain open for long periods of time and flicker between the open and closed states.

The ensemble average of 64 such sweeps at the same potential is shown in Fig. 5B. The ensemble current is characterized by a rapid rise to peak followed by a decay to steady-state levels, similar to the macroscopic currents from cells expressing H4 RNA shown in Fig. 1C. The unitary currents are binomially distributed around a mean of 1.1 pA giving an apparent single-channel conductance of 11 pS. From measurements of unitary conductance at various potentials we estimate a single-channel conductance of 10–13 pS.

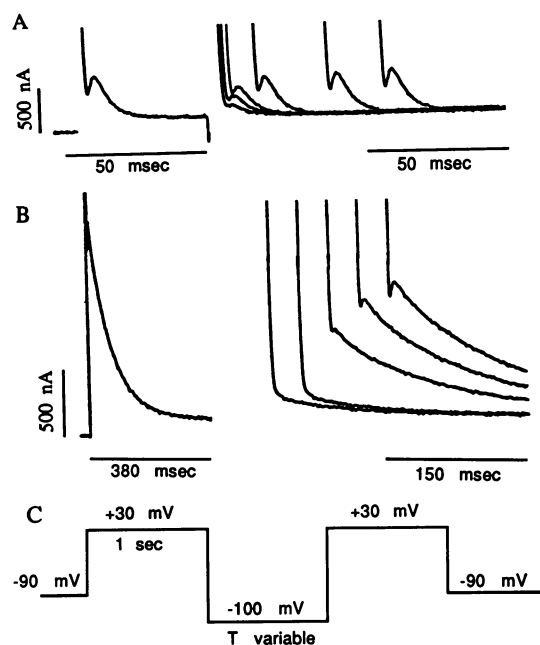


FIG. 4. Recovery from inactivation of currents from cells expressing H4 (A) and H37 (B) RNAs at room temperature (22°C). The pulse protocol used is shown in C. The interpulse intervals (T variable) were 10, 22, 44, 165, 670, and 1500 ms for H4 and 115, 280, 670, 1000, and 1500 ms for H37. In both cases the duration of the first pulse was 1 s although only the early time course is shown here.

## DISCUSSION

**Structure-Function Relationships of *Sh* K<sup>+</sup> Channels.** Four *Sh* RNAs have been expressed in *Xenopus* oocytes: two in this study (H4 and H37) and two in an independent report (ShA1 and ShB1; ref. 18). The predicted proteins encoded by these RNAs are identical throughout a region of 388 amino acids and differ in their amino and carboxyl domains (11, 13, 14). The channels expressed by these RNAs are K<sup>+</sup> selective (this report and ref. 18). A comparison of other properties (Table 1) suggests that the channel pore and gating machinery are formed by structures in the conserved region of the polypeptides, resulting in similar ionic selectivity and voltage dependence of activation and inactivation. Consistent with this possibility is the fact that the conserved region of the four polypeptides includes most of the presumptive membrane-spanning domains and the S4-like sequence.

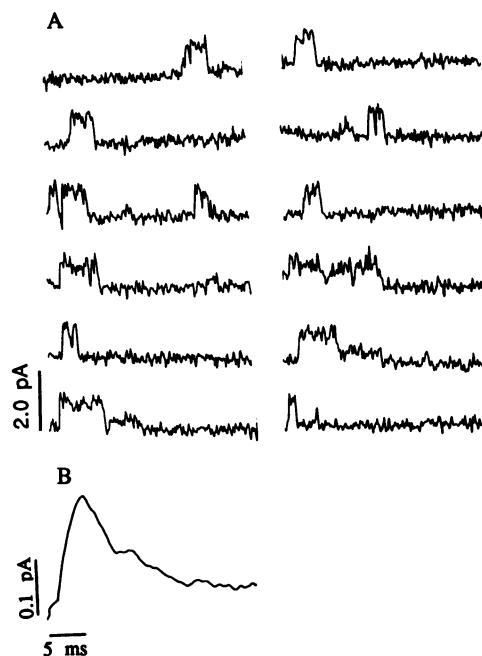


FIG. 5. Single A channels recorded in an outside-out patch from an oocyte injected with H4 RNA. (A) Twelve representative sweeps containing channel openings during the test pulse are shown. Holding potential, -80 mV; test potential, +20 mV; pulse duration, 30 ms; interval between pulses, 5 s. About 15% of the sweeps contained no channel openings (data not shown). Leak and uncompensated capacitance was digitally subtracted from each sweep by using the average of several sweeps containing no channel openings. The data were filtered at 2 kHz. (B) Ensemble average of 64 consecutive sweeps digitally filtered at 800 Hz.

The H4 and ShB1 cDNAs have the same 5' and 3' ends and presumably encode identical polypeptides. Consistent with this, their expressed currents are similar. ShA1 and H4 (or ShB1) RNA-induced currents differ markedly in the rate of recovery from inactivation, and perhaps in their rates of inactivation. The predicted proteins encoded by ShA1 and H4 RNAs have identical amino domains but different carboxyl termini. This structural difference is presumably the major determinant of the functional differences (18). H37 and ShA1 RNA-induced currents are similar in their characteristic slow recovery from inactivation although a more quantitative comparison requires further data. However, the currents appear to differ dramatically in the rates of devel-

Table 1. Properties of K<sup>+</sup> currents expressed in oocytes injected with *Sh* RNAs and in *Drosophila* muscle preparations

Property	Sh RNA in oocytes				Muscle A channel		
	H4 (II/iv)	H37 (III/i)	ShA1 (II/i)	ShB1 (II/iv)	Embryonic	Larval	Pupal
Activation voltage, mV	-40 to -30	-40 to -30	-40 to -30	-40 to -30	-30	-30	-40
4-AP sensitivity (at 5 mM), %	100	100	70	70	100	—	100
Midpoint of inactivation, mV	-35	-35	—	—	-30	-40	-40
Steepness of inactivation, mV/ <i>e</i> -fold	4.5	4.5	—	—	4.5*	4.5	—
Steepness of conductance, mV/ <i>e</i> -fold	6.5	5.5	—	—	—	6	—
Time to peak at +20 mV, ms	4	10	—	—	2.8*	2-3	3.5
$\tau$ inactivation at -10 mV, ms	6.5	95	20	12	—	6.7	—
$\tau$ inactivation at +40 mV, ms	3	60	7.8	4	≈3*	—	—
Single-channel conductance, pS	10-13	—	—	—	12-16	—	—

The 5' and 3' classification of *Sh* cDNAs is as described by Kamb *et al.* (13) from published sequences (11, 13, 14). The 5' classification in uppercase roman numerals and the 3' classification in lowercase roman numerals are shown in parentheses. The 4-aminopyridine (4-AP) block of pupal A currents was done at 10 mM (8). Time constants were calculated at 20°C, assuming a Q<sub>10</sub> of 3.2 (see Fig. 1). Single-channel conductance from cells expressing H4 RNA was determined in a 90-2 mM (inside-outside) KCl gradient. Embryonic myotube single-channel conductance was determined in a 140-2 mM (inside-outside) KCl gradient (9). Further experiments are required to determine if the difference in the steepness of the conductance of H4 RNA- and H37 RNA-induced currents, and the shift shown in Fig. 3A are significant. References for muscle A-channel data are as follows: for embryonic channels, ref. 9; for larval channels, ref. 6; and for pupal channels, ref. 8.

\*W. Zagotta and R. W. Aldrich, personal communication.

opment of activation and inactivation (Table 1). The predicted proteins encoded by these two RNAs differ only in their amino domains. This suggests that amino-terminal domains can also affect channel kinetics.

**Comparison of *Drosophila* Muscle A Currents and *Sh* A Currents Expressed in *Xenopus* Oocytes.** Currents in oocytes expressing H4 RNA are remarkably similar to those of *Drosophila* muscle A channels (Table 1). Although a quantitative comparison of the recovery from inactivation is not possible because the experiments were done at different membrane potentials, the available data suggest that the currents from cells expressing H4 RNA and the *Drosophila* muscle A currents also have similar kinetics of recovery from inactivation (6–8). These results suggest that *Drosophila* muscle A channels may be composed of H4-like gene products alone.

In contrast, the currents from cells expressing H37 or ShA1 RNAs recover extremely slowly from inactivation. This is unlike any previously reported K<sup>+</sup> channels indicating that they may represent an unusual channel type. Alternatively ShA1 and H37 polypeptides may only exist in heteromultimers in *Drosophila* (see below) or undergo some kind of modulation that does not take place in the oocytes.

The injection of E1 or H2 RNAs in oocytes does not induce K<sup>+</sup> currents when injected alone, so the function of these “short” RNAs (class iii 3' ends) remains unclear. It is unlikely that these cDNAs were generated by a cloning artifact or incomplete processing of the primary transcript (14) since three distinct Sh cDNAs with class iii 3' ends have been isolated from three different libraries (12, 13). Although the short class iii polypeptides may function in any number of ways, one attractive possibility is that they exist only in a heteromultimeric complex with long Sh products (class i, ii, or iv) to provide additional modulation of channel properties.

***Sh* K<sup>+</sup> Channel Structure.** The Na<sup>+</sup> channel is composed of four homologous domains each containing several potential membrane-spanning hydrophobic regions and one S4 region (15). These homologous domains presumably function as pseudosubunits in the formation of the channel, where a transmembrane pore is formed at the center of the symmetrical array of homologous structural units (15–17). The structural similarity between the Sh polypeptides and each of the homologous domains of the Na<sup>+</sup> channel suggests that the functional Sh K<sup>+</sup> channel is a multimer formed by the interaction of Sh polypeptides. From the steepness of the conductance (Table 1), we calculate a minimum equivalent gating charge of between 3.5 and 4.5 for the H4 and H37 channels (see p. 55 of ref. 2). A multimer containing two to four subunits will be consistent with models in which the rotation of each S4 helix results in the transfer of between one and two charges across the membrane (15–17).

Gene-dosage and complementation analyses of *Sh* mutations suggest that the functional A channel in *Drosophila* larval muscle is a heteromultimer (21). Our results indicate that a heteromultimer is not strictly required since a single *Sh* gene product suffices to form functional A channels in oocytes. Although complex, a preliminary analysis of the properties of currents expressed following injection of a 1:1 mixture of H4 and H37 RNA indicates that a third component(s) that inactivates and recovers from inactivation with time courses intermediate to the currents from cells expressing H4 and H37 RNAs (i.e., a hybrid channel) is also expressed in these oocytes.

**Types of K<sup>+</sup> Channels Encoded at the *Sh* Locus.** A variety of fast, transient voltage-dependent K<sup>+</sup> currents have been described in several species (1). Although all are called A channels they show considerable variability in the voltage-

dependence and kinetics of activation and inactivation. The observations made on Sh cDNA expression indicate that, for the family of channels encoded in the *Sh* locus, voltage dependence is a more constant parameter. This suggests that differences in the voltage dependence of activation and inactivation may be one useful way to catalog various A channels. One category (“subclass”) includes A channels that activate at relatively positive potentials (–40 to –20 mV) and show significant inactivation in a similar voltage region. This includes all A channels normally encoded by the *Sh* locus: muscle A channels (6, 7), myocyte A1 channels (9), and the channels expressed from Sh RNAs (this report and ref. 18). This subclass may also include A channels in other cells (see table 4 in ref. 1). A second category includes channels that begin to activate at more negative potentials (–70 to –50 mV) and also inactivate in this voltage region. The voltage-dependent properties of these latter A channels indicate that they operate in the subthreshold region for Na<sup>+</sup> action potential generation. These channels have been seen in *Drosophila* neurons (A2 channels; ref. 9) as well as molluscan and mammalian neurons and other cell types (1).

Solc *et al.* (9) have shown that mutations of the *Sh* locus affect only the A1 channel. Together with the results of the oocyte expression experiments these results indicate that, although different chromosomal genes encode different A channels, additional diversity for *Sh*-encoded A channels is generated by an alternative splicing mechanism.

We thank D. Krafte for his expert advice in oocyte patch clamping, and J. Campanelli, A. Kamb, M. Mathew, J. D. Pollock, and M. Ramaswani for their comments. This research was supported by U.S. Public Health Service Grants GM26976 to B.R.; NS21327 to M.A.T., GM10991 to N.D., NS11756 to H.A.L., and a Pfeiffer Research Foundation grant to M.A.T.

1. Rudy, B. (1988) *Neuroscience* **25**, 729–750.
2. Hille, B. (1984) *Ionic Channels of Excitable Membranes* (Sinauer, Sunderland, MA).
3. Llinas, R. (1984) in *Brain Slices*, ed. Dingleline, R. (Plenum, New York), pp. 7–24.
4. Adams, P. R. & Galvan, M. (1986) *Advances in Neurology*, eds. Delgado-Escueta, A. V., Ward, A. A., Jr., Woodbury, D. M. & Porter, R. J. (Raven, New York), Vol. 44, pp. 137–170.
5. Klein, M., Camardo, J. & Kandel, E. R. (1982) *Proc. Natl. Acad. Sci. USA* **79**, 5713–5717.
6. Wu, C.-F. & Haugland, F. N. (1985) *J. Neurosci.* **5**, 2626–2640.
7. Salkoff, L. & Wyman, R. J. (1983) *J. Physiol. (London)* **337**, 687–709.
8. Salkoff, L. (1983) *Cold Spring Harbor Symp. Quant. Biol.* **48**, 221–231.
9. Solc, C. K., Zagotta, W. N. & Aldrich, R. W. (1987) *Science* **236**, 1094–1098.
10. Kamb, A., Iverson, L. E. & Tanouye, M. A. (1987) *Cell* **50**, 405–413.
11. Tempel, B. L., Papazian, D. M., Schwartz, T. L., Jan, Y. N. & Jan, L. Y. (1987) *Science* **237**, 770–775.
12. Baumann, A., Krah-Jentgens, I., Mueller, R., Mueller-Holtkamp, F., Seidel, R., Kecskemethy, N., Casal, J., Ferrus, A. & Pongs, O. (1987) *EMBO J.* **6**, 3419–3429.
13. Kamb, A., Tseng-Crank, J. & Tanouye, M. A. (1988) *Neuron*, in press.
14. Schwarz, T. L., Tempel, B. L., Papazian, D. M., Jan, Y. N. & Jan, L. Y. (1988) *Nature (London)* **331**, 137–142.
15. Noda, M., Ikeda, T., Kayano, T., Suzuki, H., Takeshima, H., Kurasaki, M., Takahashi, H. & Numa, S. (1986) *Nature (London)* **320**, 188–192.
16. Guy, H. R. & Seetharamulu, P. (1986) *Proc. Natl. Acad. Sci. USA* **83**, 508–512.
17. Catterall, W. A. (1986) *Annu. Rev. Biochem.* **55**, 953–985.
18. Timpe, L. C., Schwarz, T. L., Tempel, B. L., Papazian, D. M., Jan, Y. N. & Jan, L. Y. (1988) *Nature (London)* **331**, 143–145.
19. Krieg, P. & Melton, D. A. (1984) *Nucleic Acids Res.* **12**, 7057–7070.
20. Krafte, D. S., Snutch, T., Leonard, J., Davidson, N. & Lester, H. A. (1988) *J. Neurosci.*, in press.
21. Haugland, F. N. & Wu, C.-F. (1988) *J. Neurosci.*, in press.